Journal of the Energy Institute 94 (2021) 157–166

Contents lists available at ScienceDirect

Journal of the Energy Institute

journal homepage: www.journals.elsevier.com/journal-of-the-energy-institute

Chemical looping gasification of biochar to produce hydrogen-rich syngas using Fe/Ca-based oxygen carrier prepared by coprecipitation

Zhifeng Hu[*,1], Zhenwu Miao [1], Haonan Chen, Jiawei Wu, Wencheng Wu, Yongzhi Ren[**], Enchen Jiang[***]

Key Laboratory for Biobased Materials and Energy of Ministry of Education, College of Materials and Energy, South China Agricultural University, Guangzhou, 510642, China

ARTICLE INFO

Article history:
Received 27 October 2020
Received in revised form
3 December 2020
Accepted 7 December 2020
Available online 9 December 2020

Keywords:
Biochar
Hydrogen
Syngas production
Chemical looping gasification
Coprecipitation preparation

ABSTRACT

Biochar chemical looping gasification (CLG) is a novel technology to obtain hydrogen-rich syngas, high gasification efficiency and low carbon deposition. This study investigates the effect of preparation methods, Fe loadings, active components, Ca loadings and steam/biochar (S/C) to achieve the optimal oxygen carrier. The results show that coprecipitation is the best preparation method to gain highest efficiency, redox activity and dispersion. H_2 production increases visibly with the increase of Fe loading, while efficiencies increase firstly and then decrease. There is an evident effect of active component on CLG. Oxygen carrier based on Fe/Ca performs a lower carbon deposition, higher H_2 production and efficiency. With the increase of Ca loading, H_2 production and efficiencies increase firstly and then decrease. S/C has an obvious effect on CLG performance. 1.5 is the optimal S/C to achieve high H_2 concentration of 67.35%, the highest gas production of 1.34 Nm^3/kg and gasification efficiency of 96.93%.

1. Introduction

As an energy of environmentally friendly and high energy density, hydrogen is considered to be an alternative to fossil fuel in the fields of heating, electricity and transportation [1,2]. With the development and application of industrial production and hydrogen fuel cell vehicles in recent years, more and more researchers in industry and scientific institutions pay attention to hydrogen production [3,4]. However, most of hydrogen is currently supplied with by-products in the conversion process of fossil fuel [5]. Moreover, hydrogen production by water electrolysis will consume excessive energy [6]. Therefore, it is necessary to efficiently produce hydrogen from renewable energy [7].

Biochar is the by-product of biomass pyrolysis for bio-oil, which is renewable, environmentally friendly and low cost [8]. After pyrolysis, biochar is rich in pore structure with less impurities [9]. Meanwhile, it will not exist the tar problems during the thermal conversion process of biochar [10]. Biochar is an excellent raw material in gasification, which can be converted into syngas through gasification or reforming technology [11]. Therefore, biochar has the potential to produce hydrogen-rich syngas in a renewable way.

Chemical looping gasification (CLG) is a novel and efficient technology for hydrogen production. The oxygen is absorbed by oxygen carrier in the air reactor to form the lattice oxygen, generating the oxidized oxygen carrier [12]. The lattice oxygen of oxygen carrier is provided to fuel after transporting into the fuel reactor, producing syngas [13]. After losing lattice oxygen, the reduced oxygen carrier is produced and then returned to the air reactor for the next cycle. The ratio of H_2 and CO (H_2/CO) can be controlled quantitatively by adjusting the proportion of fuel, steam and oxygen carrier [14]. Thus, the syngas produced by CLG will obtain a wide range of applications [15]. In addition, oxygen carrier also provides catalysis to promote the reaction during CLG [16]. Therefore, more and more researchers focus on the study of chemical looping process to produce syngas or hydrogen-rich syngas [17–19].

Owing to the advantages of low cost, environmental friendliness, high carbon conversion, good mechanical strength and reaction performance, Fe-based oxygen carrier has become an important oxygen carrier in CLG [20,21]. Hematite is used as oxygen

* Corresponding author.
** Corresponding author.
*** Corresponding author.
E-mail addresses: huzf@scau.edu.cn (Z. Hu), renyongzhi@scau.edu.cn (Y. Ren), enchenjiang01@163.com (E. Jiang).
[1] Zhifeng Hu and Zhenwu Miao contributed equally.

https://doi.org/10.1016/j.joei.2020.12.006
1743-9671/

carrier in CLG of lignite, indicating that Fe_2O_3 of hematite promotes lignite conversion to syngas after CLG without serious sintering [22]. The CLG of microalgae is conducted by using single Fe_2O_3 oxygen carrier, revealing that oxygen carrier content and temperature will affect the syngas production and efficiency, meanwhile Fe_2O_3 will sinter at high temperature [23]. Fe_2O_3/Al_2O_3 prepared by impregnation method is used as oxygen carrier in a continuous biomass CLG, which obtaines a syngas of 37% H_2, 21% CO, 34% CO_2 and 7% CH_4, and a high reactivity with some Fe lost [24]. However, high concentration of CO_2 is indispensable. Ca can promote the tar cracking and absorb CO_2 through carbonation, improving the H_2 concentration [25]. Thus, Ca is added into Fe-based oxygen carrier to improve CLG performance by many researchers. A visible improvement of syngas production is recorded in CLG process after CaO mixed mechanically with Fe_2O_3 [15]. Fe_2O_3/CaO prepared by impregnation method is used as oxygen carrier in biomass CLG, the results indicates that this oxygen carrier has a great hydrogen selectivity but should be enhanced the cyclic durability [26].

Based on the previous studies, oxygen carrier prepared by different methods may affect the reaction performance and the interaction of oxygen carrier [27]. Most studies have focused on the reaction performance based on oxygen carrier prepared by single method, which cannot analyze the interaction between the carrier and the active component. Moreover, preparation method of oxygen carrier is a key factor worthy of further study. However, no study has investigated the comprehensive consideration of reaction performance under different preparation methods. Therefore, concerns of the above insufficiency, the objective of this study is to evaluate the oxygen carrier performance on biochar CLG under different preparation methods of oxygen carrier. To gain better insight into the performance of Fe/Ca based oxygen carrier, the effects of Fe loadings, active components, Ca loadings and steam/biochar (S/C) are studied on hydrogen-rich syngas production, CLG performance and oxygen carrier characterization. The results will be helpful for the hydrogen-rich syngas production and preparation methods of oxygen carrier on biochar CLG process.

2. Materials and methods

2.1. Materials

Biochar is used as the CLG feedstock, which is produced from the pyrolysis of camellia shell under 550 °C for 10 min. Before pyrolysis, camellia shell is grinded to obtain particles less than 20 μm. The proximate analysis, ultimate analysis and lower heating value (LHV) of biochar and camellia shell are shown in Table 1. After grinding and sieving, the particle size of biochar is less than 200 μm.

Four preparation methods for oxygen carrier are conducted in this study.

1) Single Fe_2O_3 method: the analytical purity Fe_2O_3 is calcined at 900 °C for 4 h, and then is grinded to attain the oxygen carrier with a particle size less than 200 μm.
2) Fe_2O_3/Al_2O_3 mechanical blending method: the analytical purity Fe_2O_3 and Al_2O_3 with a molar ratio of Fe:Al = 1:2 are mechanically blended. They are calcined at 900 °C for 4 h, and then grinded to attain the oxygen carrier with a particle size less than 200 μm.
3) Impregnation method: based on the molar ratio of Fe:Al = 1:2, Al_2O_3, $Fe(NO_3)_3$•$9H_2O$ and 100 mL deionized water are placed in a beaker and stirred at 65 °C for 2 h. After dried at 105 °C for 12 h, the sample is calcined at 400 °C for 2 h and 900 °C for 4 h. And then the sample is grinded to attain the oxygen carrier with a particle size less than 200 μm.
4) Coprecipitation method: under different molar ratios of active components (Fe, Cu, Mn, Ca):Ca:Al, nitrate solutions of active components, $Ca(NO_3)_2$•$4H_2O$, $Al(NO_3)_3$•$9H_2O$ and 100 mL deionized water are dissolved in a beaker. During stirring at 25 °C, 1 mol/L ammonium carbonate solution is added slowly into the mixture until the solution changes into a colloidal suspension. After dried at a vacuum drying oven at 105 °C for 12 h, the sample is calcined at 400 °C for 2 h and 900 °C for 4 h. And then the sample is grinded to attain the oxygen carrier with a particle size less than 200 μm.

According to our previous studies [14,28], 1.5 is the optimal ratio of active component/feedstock to obtain high efficiencies and syngas production. Therefore, a certain amount of oxygen carrier/biochar with this ratio are mixed evenly by a stirrer in this study.

2.2. Experimental procedure

In this paper, the CLG experiments are conducted in a fixed bed reactor. Before experiment, 99.99% N_2 is ventilated into the fixed bed reactor for 20 min to maintain the inert atmosphere. After maintained at 800 °C, 5 g sample is placed into the center of the fixed bed reactor for 30 min. Meanwhile, distilled water with a certain flow rate is injected into the fixed bed reactor. During experiment, the flue gas is measured by Gas Chromatograph after condensation. After CLG, the reduced oxygen carrier is detected by SEM, XRD, BET, TG and O_2-TPO.

The calculations of four evaluation parameters are shown in our previous paper [29], including gas production, LHV, gasification efficiency and carbon conversion efficiency.

3. Results and discussion

3.1. Effects of preparation methods on CLG

In this section, four preparation methods of oxygen carrier (single Fe_2O_3 method, Fe_2O_3/Al_2O_3 mechanical blending method,

Table 1
The proximate analysis, ultimate analysis and LHV of biochar and camellia shell.

Proximate analysis[a] (wt, %)			Ultimate analysis[b] (%)			LHV (MJ/kg)	
	Biochar	Camellia shell		Biochar	Camellia shell	Biochar	Camellia shell
M	5.04	15.66	C	73.79	38.50	22.14	15.95
A	9.68	2.90	H	3.78	4.16		
V	14.76	64.70	O[c]	12.03	38.03		
FC	70.52	16.75	N	0.70	0.42		
			S	0.02	0.33		

[a] On wet basis.
[b] On dry ash free basis.
[c] Calculated by difference.

impregnation method and coprecipitation method) are studied to obtain the effects on CLG performance under a molar ratio of Al:Fe = 2:1 and S/C of 0.5.

The effect of preparation methods on gas concentration and gas production is shown in Fig. 1(a). The trends of gas concentration are similar under four methods. The highest is H_2 (61.53%–65.18%), followed by CO_2 (21.99%–25.70%) and CO (6.51%–11.75%). The lowest is CH_4 (only 2.10%–2.95%). This phenomenon is mainly because 1) water-gas shift reaction ($CO + H_2O \rightarrow H_2 + CO_2$) and carbon gasification reaction ($C + H_2O \rightarrow H_2 + CO$, $C + CO_2 \rightarrow 2CO$) are enhanced with the help of steam, resulting in the highest H_2 concentration and more than twice that of CO_2. 2) under the supply of lattice oxygen by oxygen carrier, part of C/CO will be converted into CO_2, thus CO concentration is lower than that of CO_2. 3) in CLG, CH_4 is mainly produced by biochar pyrolysis process. As shown in Table 1, a low content of H (only 3.78%) and volatile (14.76%) lead to the lowest CH_4 concentration.

However, gas production is different among four methods. The highest is coprecipitation method (0.93 Nm^3/kg), followed by impregnation method (0.76 Nm^3/kg) and single Fe_2O_3 method (0.73 Nm^3/kg), while Fe_2O_3/Al_2O_3 mechanical blending method (0.70 Nm^3/kg) is the lowest. As a physical process, the dispersion structure will hinder the release of lattice oxygen under the mechanical blending method [22]. Therefore, gas production of this method is the lowest, even lower than that of single Fe_2O_3 method. However, as shown in the XRD results of Fig. 1(b), Fe_2O_3 is reduced into FeO under single Fe_2O_3 method after CLG process. FeO is believed to easily form agglomeration and sintering [23], resulting in a low gas production under single Fe_2O_3 method. In addition, as a chemical process, the active component Fe will be evenly distributed on Al_2O_3, leading to a high gas production under coprecipitation and impregnation method. Furthermore, as shown in the XRD results of Fig. 1(b), wider diffraction peaks are detected under coprecipitation method, indicating that oxygen carrier of this method has a higher dispersion and a smaller particle. Further, $FeAl_2O_4$ with a better crystal structure and thermal stability [30] is detected under coprecipitation method after CLG process, which illustrates that all Fe^{3+} are reduced into Fe^{2+}, achieving a complete redox ability without sintering. Moreover, as shown in Table 2, a smaller surface area and porosity is detected under coprecipitation method, which is conducive to the uniform distribution and stronger combination between carrier and active component [31]. Therefore, oxygen carrier prepared by coprecipitation method has a highest performance in gas production.

The effect of preparation methods on efficiency and LHV is shown in Fig. 1(c). There is a positive correlation between LHV and the concentration of combustible gas (H_2, CO and CH_4) based on the formulation of LHV. The highest concentration of combustible gas is obtained under coprecipitation method (78.01%), followed by impregnation method (76.12%). Therefore, the highest LHV is coprecipitation method (14.30 MJ/Nm^3), followed by impregnation method (14.24 MJ/Nm^3). And the lowest is single Fe_2O_3 method (13.75 MJ/Nm^3).

As shown in Fig. 1(c), the lowest carbon conversion efficiency (30.33%) and gasification efficiency (44.78%) are obtained under Fe_2O_3/Al_2O_3 mechanical blending method because the release of lattice oxygen from Fe_2O_3 is weakened by the obstruction of carrier Al_2O_3 under mechanical blending, sacrificing partial efficiency to prevent the deep reduction of Fe_2O_3 and alleviate sintering of oxygen carrier [32]. The carbon conversion efficiency (34.48%) and gasification efficiency (45.46%) of single Fe_2O_3 method are slightly higher than that of mechanical blending method, but the sintering caused by the deep reduction under this method is not conducive to long-term cycle reaction. Among these four preparation methods, the highest carbon conversion efficiency (40.68%) and gasification efficiency (60.06%) are obtained under coprecipitation method, followed by impregnation method (36.81% and 50.49%). This is mainly because smaller surface area and porosity are detected as shown in Table 2, indicating the uniform distribution and combination between carrier and Fe_2O_3 are better in these two methods. Moreover, compared with the single Fe_2O_3 and mechanical blending method, oxygen carriers have a higher dispersion and smaller particles under these two methods because wider diffraction peaks are shown in Fig. 1(b). In addition, according to the XRD result, $FeAl_2O_4$ behaves a better crystal structure and the carrier Al_2O_3 behaves a more prominent effect under these two methods. As a result, better carbon conversion efficiency and gasification efficiency are obtained under coprecipitation and impregnation method. Furthermore, the interaction between the active component Fe and carrier is stronger under coprecipitation method [31], obtaining a better reaction performance. Further, two peaks of Fe_2O_3 reduction [33] are shown in Fig. 1(d) under these two methods. Meanwhile, an earlier and more hydrogen consumption is detected under coprecipitation method, which indicates that oxygen carrier of coprecipitation method presents a stronger Fe_2O_3 reduction and higher O_2 release performance, resulting in a higher and easier redox activity. In addition, as shown in Fig. 1(e), after CLG, smaller particles and more evenly dispersion are observed under coprecipitation method, which is consistent with the XRD results. However, a slight sintering and inferior dispersion are observed under impregnation method. Therefore, oxygen carrier of coprecipitation method has a better performance in CLG.

Based on the comprehensive consideration, the best oxygen carrier preparation method is coprecipitation method for CLG in this study.

3.2. Effects of Fe loadings on CLG

According to the discussion of section 3.1, coprecipitation method is chosen for oxygen carriers preparation in the following sections. In order to investigate the optimal Fe loading, the effect of Fe loadings prepared on carrier is studied with a S/C of 0.5 in this section under the molar ratios of Fe:Al = 0.5:2, 1:2, 1.5:2, 2:2 and 2.5:2, respectively.

The effect of Fe loadings on gas concentration is shown in Fig. 2(a). With the increase of Fe:Al from 0.5:2 to 2.5:2, the concentration of H_2 and CO_2 increases respectively by 8.50% and 3.85%, while the concentration of CO and CH_4 decreases accordingly. This phenomenon is mainly because 1) there is more active component Fe_2O_3 loaded on carrier Al_2O_3 with the increase of Fe loading. As a catalyst, more active component shows stronger catalytic effect, promoting the water-gas shift reaction ($CO + H_2O \rightarrow H_2 + CO_2$), carbon gasification reaction ($C + H_2O \rightarrow H_2 + CO$) and reforming reaction ($CH_4 + H_2O \rightarrow 3H_2 + CO$) during CLG process. Thus, higher Fe loading produces more H_2. 2) with the increase of Fe loading, Fe_2O_3 provides adequate oxygen and enhances the reactions of $CO + Fe_2O_3 \rightarrow CO_2 + Fe_3O_4$, $CH_4 + 4Fe_2O_3 \rightarrow 2H_2O + CO_2 + 8FeO$and $C + 2Fe_2O_3 \rightarrow CO_2 + 4FeO$[23,34], leading to an increase of CO_2 and decrease of CO and CH_4.

As shown in Fig. 2(a), with the increase of Fe:Al from 0.5:2 to 2.5:2, gas production increases firstly and then decreases, obtaining the highest gas production of 1.09 Nm^3/kg at 1.5 Fe loading. With the increase of Fe:Al from 0.5:2 to 1.5:2, the increase of active component Fe_2O_3 provides more lattice oxygen and catalytic effect, strengthening the gasification reaction and gas production. However, gas production decreases when Fe:Al increases from 1.5:2 to 2.5:2. It is mainly because 1) the BET surface area increases continually from 6.35 m^2/g to 11.51 m^2/g when Fe:Al increases from 0.5:2 to 2.5:2, which indicates that the distribution of particles is uneven and the combination between Fe_2O_3 and Al_2O_3 becomes

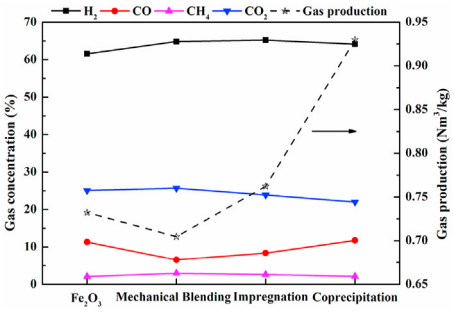

(a) Gas concentration and production

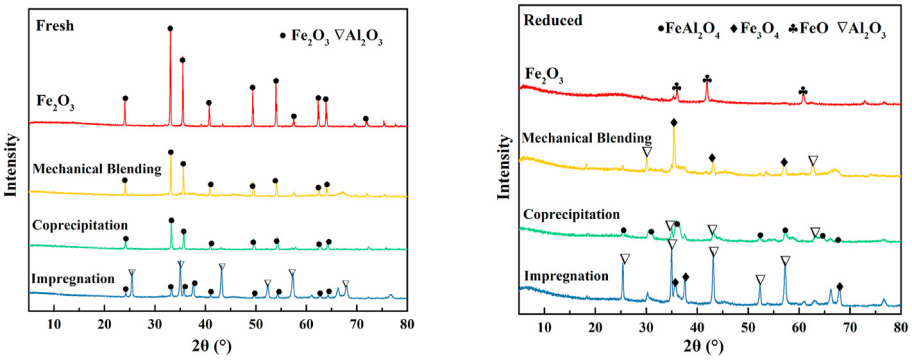

(b) XRD of fresh and reduced oxygen carrier

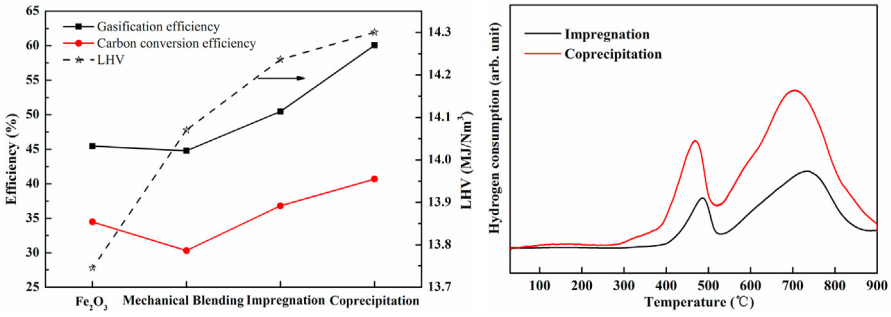

(c) Efficiency and LHV (d) H_2-TPR

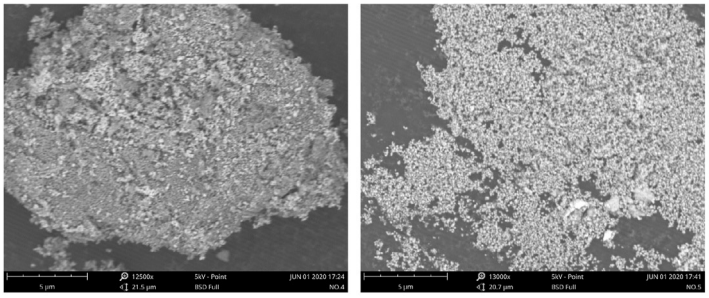

Impregnation Coprecipitation

(e) SEM

Fig. 1. The effect of preparation methods on CLG performance.

Table 2
The effect of preparation methods on surface area and pore structure.

Methods	Surface Area (m^2/g)	Pore Volume (cm^3/g)
$SiO_2 + Fe_2O_3$	134.42	0.093
Mechanical blending	44.63	0.120
Impregnation	20.28	0.052
Coprecipitation	7.27	0.012

weaker [31]. 2) as shown in the XRD results of Fig. 2(b), with the increase of Fe loading, the intensity of Fe_2O_3 increases accordingly while the intensity of Al_2O_3 decreases obviously. This XRD analysis reveals that more Fe_2O_3 covers on Al_2O_3, weakening the support effect of carrier Al_2O_3. 3) as shown in the H_2-TPR results of Fig. 2(c), with the increase of Fe loading, the temperature of hydrogen consumption peaks becomes higher, which means that Fe_2O_3 reduction and O_2 release become harder and need more energy to react under higher Fe loading condition. In other words, high Fe loading weakens the interaction between Fe_2O_3 and carrier Al_2O_3. Therefore, the excessive Fe loading exceeds the carrier capacity, weakening the CLG and oxygen carrier performance. Thereinto, moderate Fe loading is conducive to particles distribution, support effect and interaction of carrier Al_2O_3.

The effect of Fe loadings on efficiency is shown in Fig. 2(d). With the increase of Fe:Al from 0.5:2 to 2.5:2, gasification efficiency and carbon conversion efficiency increase firstly and then decrease, obtaining the highest gasification efficiency of 70.57% and carbon conversion efficiency of 46.77% at 1.5 Fe loading. When Fe:Al increases from 0.5:2 to 1.5:2, the increase of Fe_2O_3 strengthens the catalytic effect and provides more lattice oxygen, promoting the conversion of biochar to gas. Thus, gasification and carbon conversion efficiency increase in these conditions. However, with the increase of Fe:Al from 1.5:2 to 2.5:2, the excessive Fe loading causes uneven distribution of particles, insufficient support and weaker interaction of carrier, inhibiting the biochar conversion and oxygen carrier performance. Therefore, gasification efficiency and carbon conversion efficiency decrease when Fe_2O_3 exceeds the moderate loading.

Based on the comprehensive consideration of CLG performance in gas concentration, gas production, oxygen carrier and efficiencies, the optimal Fe loading in oxygen carrier is Fe:Al of 1.5:2 in this study.

3.3. Effects of active components on CLG

Based on the discussion of above sections, four active components (Cu, Mn, Ca and Fe) loaded on Al_2O_3 are prepared by coprecipitation method with a molar ratio of active component/Al = 1.5:2 and a S/C of 0.5, investigating the performance of active component on CLG and oxygen carrier in this section.

As shown in Fig. 3(a), Cu-based oxygen carrier has the lowest concentration of H_2 and CH_4 (52.40% and 1.23%) and the highest concentration of CO and CO_2 (14.95% and 31.43%). Due to the high oxygen transport capacity and reactivity [35], more oxygen is provided by Cu-based oxygen carrier for the biochar gasification and oxidization of H_2, CO and CH_4, producing less production of H_2 and CH_4 and more production of CO and CO_2. Compared with Cu-based oxygen carrier, because of a weaker reactivity and oxygen

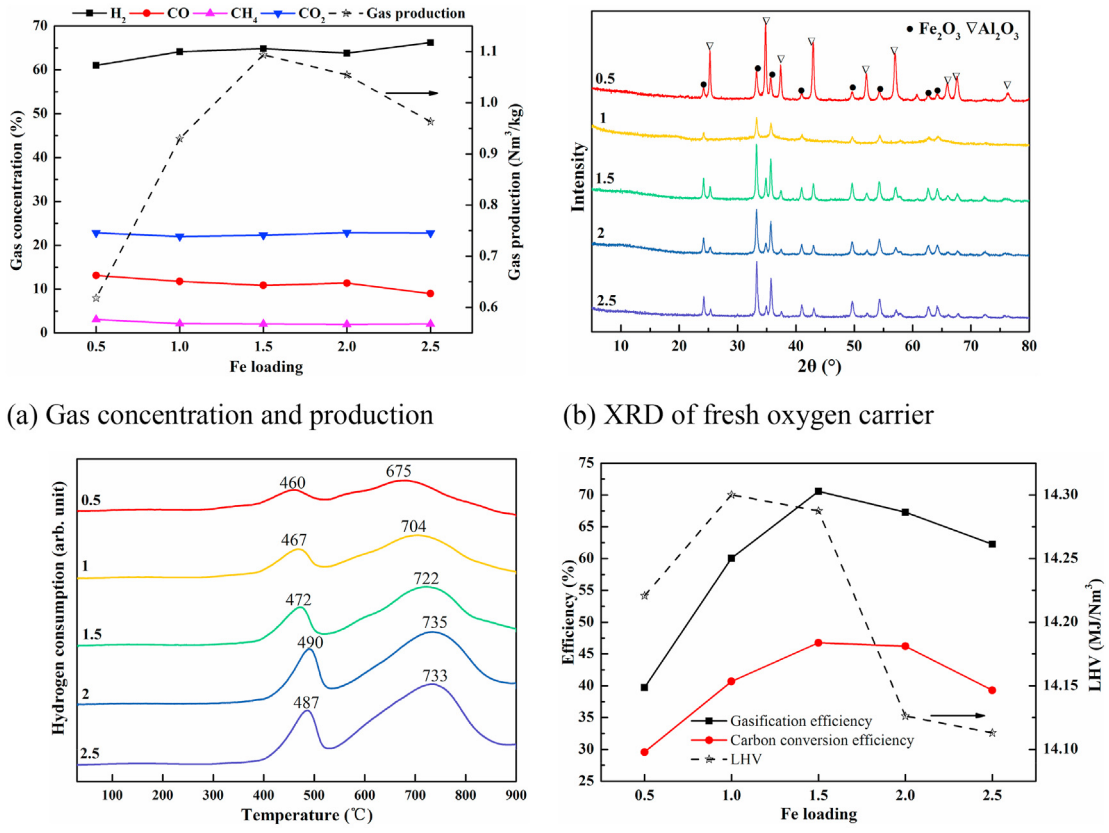

Fig. 2. The effect of Fe loadings on CLG performance.

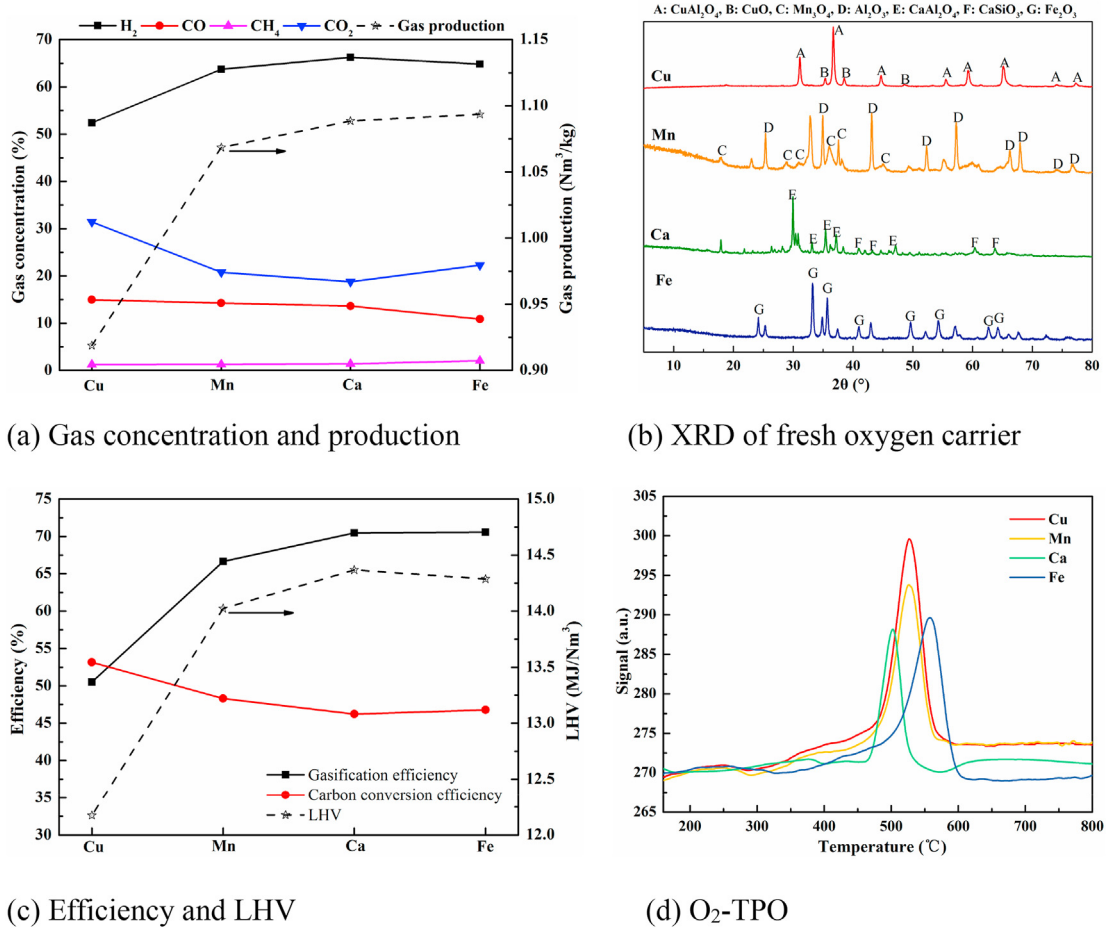

Fig. 3. The effect of active components on CLG performance.

transport capacity of Mn-based oxygen carrier, less biochar and H_2 are converted into gas and H_2O, producing less CO and CO_2, but more H_2. The H_2 concentration of Ca-based oxygen carrier is the highest (66.26%), followed by Fe-based oxygen carrier (64.82%), which indicates that Ca- and Fe-based oxygen carrier are conducive to the formation of H_2-rich syngas. Thereinto, owing to a strong performance of CO_2 capture [36], the CO_2 concentration of Ca-based oxygen carrier is the lowest (18.74%), increasing accordingly the H_2 concentration.

The highest gas production is obtained from Fe-based oxygen carrier (1.09 Nm^3/kg), followed by Ca-based oxygen carrier (1.08 Nm^3/kg). This is because the active component CaO plays a role of catalyst in CLG to increase the production of CO and H_2 [37], improving the gasification efficiency and gas production [38]. Among these four active components, the lowest gas production is obtained from Cu-based oxygen carrier (0.92 Nm^3/kg). As shown in Fig. 3(b), CuO is detected in the XRD of Cu-based oxygen carrier. Substantial deactivation and sintering of Cu-based oxygen carrier occur at high temperature due to the low melting point of CuO and Cu [39]. Thus, Cu-based oxygen carrier produces a low gas production.

The effect of active components (Cu, Mn, Ca and Fe) on efficiency and LHV is shown in Fig. 3(c). The highest gasification efficiency of 70.57% is obtained from Fe-based oxygen carrier among these four active components. This is because the deep and stepwise reduction of Fe_2O_3 ($Fe_2O_3 \rightarrow Fe_3O_4 \rightarrow FeO \rightarrow Fe$) provides much lattice oxygen [23], showing high activity of oxygen carrier. Moreover, as shown in the O_2-TPO results of Fig. 3(d), low carbon deposition is detected on Fe-based oxygen carrier, indicating the strong anti-carbon deposition and reactivity performance of Fe-based oxygen carrier. Ca-based oxygen carrier displays a good gasification efficiency of 70.46%. This is mainly because the catalytic effect of Ca enhances the tar cracking, increasing the production of CO and H_2 [25]. Furthermore, as shown in the XRD results of Fig. 3(b), the detected crystals of $CaAl_2O_4$ and $CaSiO_3$ are conducive to the structure stability of oxygen carrier, promoting the continuous reaction of CLG. Further, as shown in the O_2-TPO results of Fig. 3(d), the lowest carbon deposition is detected on Ca-based oxygen carrier, revealing a perfect CLG performance. Therefore, Ca-based oxygen carrier shows a good gasification efficiency. Meanwhile, owing to a strong performance of CO_2 capture, the highest LHV of 14.37 MJ/Nm^3 is obtained from Ca-based oxygen carrier.

As shown in the O_2-TPO results of Fig. 3(d), Mn-based oxygen carrier has a higher carbon deposition than that of Fe- and Ca-based oxygen carrier, indicating a weaker sustainability and reactivity of oxygen carrier. Thus, Mn-based oxygen carrier shows a good gasification efficiency, LHV and gas production, but lower than that of Fe- and Ca-based oxygen carrier. The highest carbon conversion efficiency is obtained from Cu-based oxygen carrier because of the high oxygen transport capacity and biochar gasification reactivity [35]. However, as shown in the O_2-TPO results of Fig. 3(d), the highest carbon deposition is detected on Cu-based oxygen carrier, covering partially the active site on the oxygen carrier. Moreover, the low melting point of Cu/CuO is easy to cause sintering. Therefore, the high carbon deposition and sintering lead to the lowest gas production and gasification efficiency of Cu-based oxygen carrier

[40]. Meanwhile, due to the highest CO_2 production and good oxygen transport capacity, Cu-based oxygen carrier has the lowest LHV.

Based on the comprehensive consideration of CLG performance in gas concentration, gas production, oxygen carrier and efficiencies, Fe and Ca are the perfect active components in this study.

3.4. Effects of Ca loadings on CLG

According to the discussion of section 3.3, Fe and Ca-based oxygen carrier show a high gasification efficiency and hydrogen selectivity. The combination of Fe and Ca maybe exhibit a great synergistic effect on CLG performance. In order to investigate the optimal Ca loading, the effect of Ca loadings prepared on Fe-based oxygen carrier is studied with a S/C of 0.5 in this section under the molar ratios of Ca:Fe:Al = 0.25:1.5:2, 0.5:1.5:2, 1:1.5:2 and 1.5:1.5:2, respectively.

The effect of Ca loadings on gas concentration and production is shown in Fig. 4(a). With the increase of Ca loading from 0.25 to 1.5, CO concentration increases firstly and then decreases, while CO_2 concentration decreases firstly and then increases. This is mainly because the CO_2 capture and catalytic effect of Ca help to enhance CO production and reduce CO_2 production. However, as shown in the XRD results of Fig. 4(b), more FeO and less Fe_3O_4 is detected with the increase of Ca loading, indicating that Ca promotes the deep reduction of Fe_2O_3 to release more lattice oxygen, which will react with CO to produce CO_2. Therefore, the concentrations of CO and CO_2 exhibit the tendency shown in Fig. 4(a). When Ca loading increases from 0.25 to 1.5, H_2 concentration and gas production increase firstly and then decreases. On the contrary, CH_4 concentration decreases firstly and then increases. Thereinto, 1.0 Ca loading achieves the highest H_2 concentration of 64.10%, the highest gas production of 1.12 Nm^3/kg and the lowest CH_4 concentration of 1.06%. This tendency can be explained that Ca is conducive to the tar cracking, promoting more gas production and resulting in a higher H_2 concentration and lower CH_4 concentration under a high Ca loading. However, the excessive Ca loading covers partial active site of Fe, inhibiting the reactivity of Fe-based oxygen carrier. Meanwhile, as shown in the XRD results of Fig. 4(b), more FeO is detected with the increase of Ca loading, which will be easier to sinter and weaker the reaction under high temperature. Therefore, increase of CH_4 concentration, decrease of H_2 concentration and gas production are observed when Ca loading increases from 1.0 to 1.5.

The effect of Ca loadings on efficiency is shown in Fig. 4(c). The gasification efficiency and carbon conversion efficiency increase firstly and then decrease when Ca loading increases from 0.25 to 1.5. Among them, 1.0 Ca loading achieves the highest gasification efficiency of 71.83% and carbon conversion efficiency of 48.22%. The reasons can be explained as follows. Firstly, as shown in Table 3, the surface area and porosity becomes smaller when Ca loading increases from 0.25 to 1.0, which indicates that the distribution of active components becomes more uniform and the combination between carrier and active components becomes stronger [31], improving the CLG performance. However, the distribution and combination become weaker since the surface area and porosity

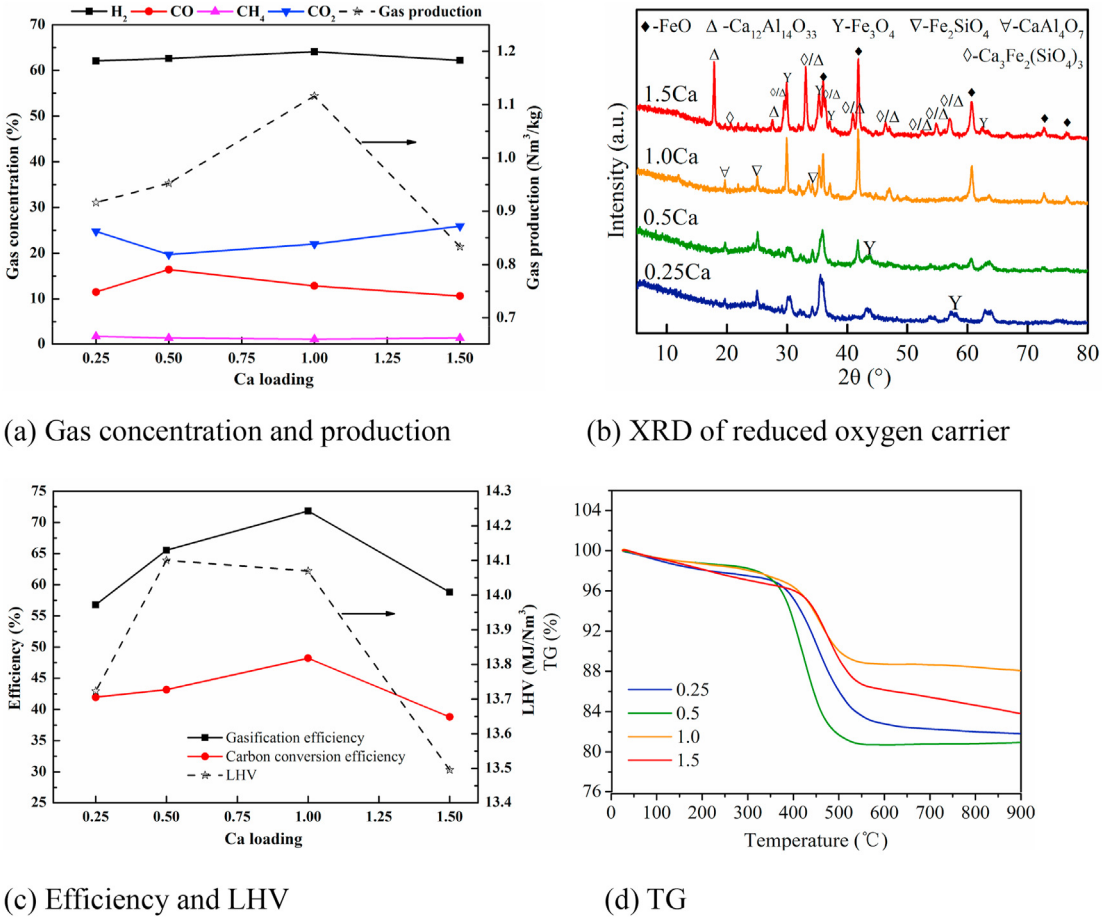

Fig. 4. The effect of Ca loadings on CLG performance.

Table 3
The effect of Ca loadings on surface area and pore structure.

Ca loadings	Surface Area (m^2/g)	Pore Volume (cm^3/g)	Pore Size (nm)
0.25	16.71	0.062	14.73
0.5	6.58	0.019	11.64
1.0	0.47	0.0008	6.53
1.5	9.29	0.020	8.82

increases under the 1.5 Ca loading, inhibiting the reactivity. Secondly, Ca can catalyze the tar cracking and biochar conversion, promoting the gasification process and gas production. Thirdly, as shown in the TG results of Fig. 4(d), many carbon deposition and unreacted biochar are observed under low Ca loadings of 0.25 and 0.5, revealing low efficiency and poor conversion. Particularly, the moderate Ca loading of 1.0 displays the lowest carbon deposition and unreacted biochar, showing a great reactivity. However, the excessive Ca loading of 1.5 increases carbon deposition and unreacted biochar, which is because the excessive Ca partially covers on Fe, weakening the conversion of active site Fe. Therefore, the gasification efficiency and carbon conversion efficiency increase firstly and then decrease with the increase of Ca loading from 0.25 to 1.5.

Based on the comprehensive consideration of CLG performance in gas concentration, gas production, oxygen carrier and efficiencies, the optimal Ca loading in Fe-based oxygen carrier is Ca:Fe:Al = 1:1.5:2 in this study.

3.5. Effects of S/C on CLG

In this section, Fe/Ca-based oxygen carrier is prepared by coprecipitation method under the molar ratio of Ca:Fe:Al = 1:1.5:2. In order to investigate the optimal S/C, the gas concentration, gas production and efficiencies are studied under the S/C of 0.25, 0.50, 0.75, 1.00, 1.25, 1.50, 1.75 and 2.00, respectively.

The effect of S/C on gas concentration is shown in Fig. 5(a). When S/C increases from 0.25 to 2.00, CO_2 and H_2 concentrations increase, while CO and CH_4 concentrations decrease. This is mainly because the increase of steam will promote the carbon gasification reaction ($C + H_2O \rightarrow H_2 + CO$), water-gas shift reaction ($CO + H_2O \rightarrow H_2 + CO_2$) and reforming reaction ($CH_4 + H_2O \rightarrow 3H_2 + CO$, $Tar + H_2O \rightarrow H_2 + CO/CO_2/CH_4$) [41] during CLG process. Therefore, the increase of S/C will increase the concentration of CO_2 and H_2 but decrease the concentration of CO and CH_4. In addition, as shown in Fig. 5(b), LHV shows an approximately increasing trend with the increase of S/C, which is positively correlated with the concentration of combustible gas.

As shown in Fig. 5, gas production, gasification efficiency and carbon conversion efficiency increase firstly and then decrease with the increase of S/C. When S/C increases from 0.25 to 1.50, gas production, gasification efficiency and carbon conversion efficiency increase obviously by 139.59%, 144.19% and 106.70%, respectively. This is because 1) the increase of steam will promote the tar cracking and biochar conversion ($Tar + H_2O \rightarrow H_2 + CO/CO_2/CH_4$ and $C + H_2O \rightarrow H_2 + CO$), producing more combustible gas. 2) after provided lattice oxygen, Fe_2O_3 converts into the reduced oxygen carrier FeO/Fe_3O_4. The increase of steam will react with the reduced oxygen carrier FeO/Fe_3O_4 to form the oxidized oxygen carrier Fe_2O_3 and convert steam into H_2 ($H_2O + FeO/Fe_3O_4 \rightarrow H_2 + Fe_3O_4/Fe_2O_3$). The oxidized oxygen carrier Fe_2O_3 will continue to provide lattice oxygen for the biochar conversion ($C + Fe_3O_4/Fe_2O_3 \rightarrow CO/CO_2 + FeO/Fe_3O_4$), increasing gas production. Therefore, gas production, gasification efficiency and carbon conversion efficiency increase obviously with the increase of S/C from 0.25 to 1.50.

However, when S/C continues to increase from 1.50 to 2.00, gas production, gasification efficiency and carbon conversion efficiency decrease clearly by 17.38%, 19.99% and 31.65%, respectively. This is mainly because 1) the excessive steam ventilates into the reactor and absorbs more heat from reactor, decreasing the reaction temperature. Thus, the excessive steam reduces the reaction performance. 2) the excessive steam will correspondingly increase the gas flow of reactor, shortening the reaction time between steam and biochar [42], which in turn leads to a decrease of gas production and efficiency. Therefore, gas production, gasification efficiency and carbon conversion efficiency decrease clearly with the increase of S/C from 1.50 to 2.00.

Based on the comprehensive consideration of CLG performance in gas concentration, gas production, oxygen carrier and efficiencies, 1.50 is the optimal S/C to achieve high H_2 concentration of 67.35% and the highest gas production of 1.34 Nm^3/kg, gasification efficiency of 96.93% and carbon conversion efficiency of 67.14% in this study.

3.6. Mechanism analysis

Fig. 6 shows the transformation of biochar and steam into H_2-rich syngas through Fe/Ca-based oxygen carrier during CLG process. Under the synergistic catalysis and lattice oxygen supply of Fe/Ca-based oxygen carrier, more biochar is converted into gas and produces less carbon deposition. Owing to the CO_2 capture, some

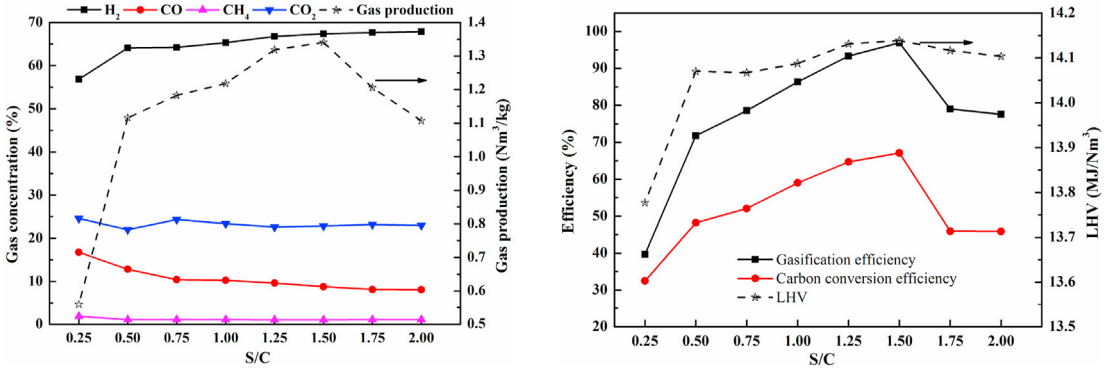

(a) Gas concentration and production (b) Efficiency and LHV

Fig. 5. The effect of S/C on CLG performance.

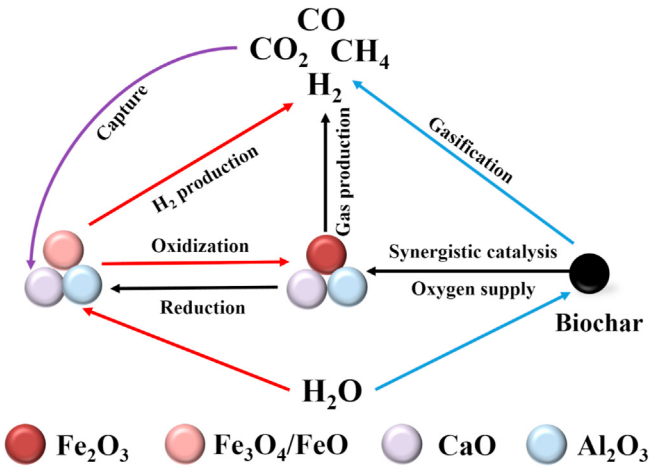

Fig. 6. Mechanism analysis.

CO_2 is captured by CaO. At the same time, Fe/Ca-based oxygen carrier is reduced into the reduced oxygen carrier. Moreover, the ventilation of steam promotes the gasification reaction of biochar, producing more syngas. Furthermore, the steam will oxidize the reduced oxygen carrier into the oxidized oxygen carrier. Meanwhile, the steam is converted into H_2. Therefore, biochar and steam can be converted into H_2-rich syngas through Fe/Ca-based oxygen carrier.

4. Conclusions

Fe/Ca-based oxygen carrier is prepared to conduct biochar CLG. Oxygen carrier prepared by coprecipitation method has a higher efficiency, stronger redox activity and better dispersion. Oxygen carrier based on Fe or Ca active components performs a lower carbon deposition, higher H_2 production and gasification efficiency. Moderate Fe loading, Ca loading and S/C are conducive to CLG performance. 1.5 and 1.0 is the optimal Fe and Ca loading to obtain highest efficiencies and lowest carbon deposition, respectively. 1.50 is the optimal S/C to achieve high H_2 concentration of 67.35%, the highest gas production of 1.34 Nm^3/kg and gasification efficiency of 96.93%.

Declaration of competing interest

The authors declare that they have no known competing financial interests or personal relationships that could have appeared to influence the work reported in this paper.

Acknowledgements

The authors are grateful to National Natural Science Foundation of China (51806068), Guangdong Natural Science Foundation (2017A030310370), Guangzhou Science and Technology Project (201804010205) and Guangdong Key Laboratory of Clean Energy Technology, China (2017B030314127) for the financial support.

References

[1] A.M. Abdalla, S. Hossain, O.B. Nisfindy, A.T. Azad, M. Dawood, A.K. Azad, Hydrogen production, storage, transportation and key challenges with applications: a review, Energy Convers. Manag. 165 (2018) 602–627.
[2] A. Darmawan, M.W. Ajiwibowo, K. Yoshikawa, M. Aziz, K. Tokimatsu, Energy-efficient recovery of black liquor through gasification and syngas chemical looping, Appl. Energy 219 (2018) 290–298.
[3] X.P. Zheng, X.S. Yuan, X.Y. Lai, R.N. Jia, Y.S. Zhu, Z.H. Zhang, et al., Hydrogen storage performance of HPSB hydrogen storage materials, Chem. Phys. Lett. 734 (2019).
[4] A.F.M. Ibrahim, K.P.R. Dandamudi, S.G. Deng, J.Y.S. Lin, Pyrolysis of hydrothermal liquefaction algal biochar for hydrogen production in a membrane reactor, Fuel 265 (2020).
[5] S. Adhikari, S.D. Fernando, A. Haryanto, Hydrogen production from glycerol: an update, Energy Convers. Manag. 50 (2009) 2600–2604.
[6] A. Tremel, P. Wasserscheid, M. Baldauf, T. Hammer, Techno-economic analysis for the synthesis of liquid and gaseous fuels based on hydrogen production via electrolysis, Int. J. Hydrogen Energy 40 (2015) 11457–11464.
[7] A.T. Wijayanta, M. Aziz, Ammonia production from algae via integrated hydrothermal gasification, chemical looping, N_2 production, and NH_3 synthesis, Energy 174 (2019) 331–338.
[8] Y. Shen, J. Wang, X. Ge, M. Chen, By-products recycling for syngas cleanup in biomass pyrolysis-An overview, Renew. Sustain. Energy Rev. 59 (2016) 1246–1268.
[9] Y. Li, B. Xing, Y. Ding, X. Han, S. Wang, A critical review of the production and advanced utilization of biochar via selective pyrolysis of lignocellulosic biomass, Bioresour. Technol. 312 (2020) 123614.
[10] D. Feng, Y. Zhang, Y. Zhao, S. Sun, J. Gao, Improvement and maintenance of biochar catalytic activity for in-situ biomass tar reforming during pyrolysis and H_2O/CO_2 gasification, Fuel Process. Technol. 172 (2018) 106–114.
[11] S. You, Y.S. Ok, S.S. Chen, D.C.W. Tsang, E.E. Kwon, J. Lee, et al., A critical review on sustainable biochar system through gasification: energy and environmental applications, Bioresour. Technol. 246 (2017) 242–253.
[12] Z. Huang, F. He, Y. Feng, K. Zhao, A. Zheng, S. Chang, et al., Synthesis gas production through biomass direct chemical looping conversion with natural hematite as an oxygen carrier, Bioresour. Technol. 140 (2013) 138–145.
[13] Y. Fan, N. Tippayawong, G. Wei, Z. Huang, K. Zhao, L. Jiang, et al., Minimizing tar formation whilst enhancing syngas production by integrating biomass torrefaction pretreatment with chemical looping gasification, Appl. Energy 260 (2020) 114315.
[14] X. Huang, J. Wu, M. Wang, X. Ma, E. Jiang, Z. Hu, Syngas production by chemical looping gasification of rice husk using Fe-based oxygen carrier, J. Energy Inst. 93 (2020) 1261–1270.
[15] Q. Liu, C. Hu, B. Peng, C. Liu, Z. Li, K. Wu, et al., High H_2/CO ratio syngas production from chemical looping co-gasification of biomass and polyethylene with CaO/Fe_2O_3 oxygen carrier, Energy Convers. Manag. 199 (2019) 111951.
[16] Z. Hu, E. Jiang, X. Ma, Microwave pretreatment on microalgae: effect on thermo-gravimetric analysis and kinetic characteristics in chemical looping gasification, Energy Convers. Manag. 160 (2018) 375–383.
[17] Z. Miao, Z. Hu, E. Jiang, X. Ma, Hydrogen-rich syngas production by chemical looping reforming on crude wood vinegar using Ni-modified HY zeolite oxygen carrier, Fuel 279 (2020) 118547.
[18] G.-Q. Wei, W.-N. Zhao, J.-G. Meng, J. Feng, W.-Y. Li, F. He, et al., Hydrogen production from vegetable oil via a chemical looping process with hematite oxygen carriers, J. Clean. Prod. 200 (2018) 588–597.
[19] J. Zeng, R. Xiao, H. Zhang, Y. Wang, D. Zeng, Z. Ma, Chemical looping pyrolysis-gasification of biomass for high H_2/CO syngas production, Fuel Process. Technol. 168 (2017) 116–122.
[20] X. Yan, J. Hu, Q. Zhang, S. Zhao, J. Dang, W. Wang, Chemical-looping gasification of corn straw with Fe-based oxygen carrier: thermogravimetric analysis, Bioresour. Technol. 303 (2020) 122904.
[21] J. Hu, C. Li, D.-J. Lee, Q. Guo, S. Zhao, Q. Zhang, et al., Syngas production from biomass using Fe-based oxygen carrier: Optimization, Bioresour. Technol. 280 (2019) 183–187.
[22] G. Wei, H. wang, W. Zhao, Z. Huang, Q. Yi, F. He, et al., Synthesis gas production from chemical looping gasification of lignite by using hematite as oxygen carrier, Energy Convers. Manag. 185 (2019) 774–782.
[23] Z. Hu, E. Jiang, X. Ma, The effect of oxygen carrier content and temperature on chemical looping gasification of microalgae for syngas production, J. Energy Inst. 92 (2019) 474–487.
[24] I. Samprón, L.F. de Diego, F. García-Labiano, M.T. Izquierdo, A. Abad, J. Adánez, Biomass Chemical Looping Gasification of pine wood using a synthetic Fe_2O_3/Al_2O_3 oxygen carrier in a continuous unit, Bioresour. Technol. 316 (2020) 123908.
[25] T. Detchusananard, K. Im-orb, P. Ponpesh, A. Arpornwichanop, Biomass gasification integrated with CO_2 capture processes for high-purity hydrogen production: process performance and energy analysis, Energy Convers. Manag. 171 (2018) 1560–1572.
[26] Q. Hu, Y. Shen, J.W. Chew, T. Ge, C.-H. Wang, Chemical looping gasification of biomass with Fe_2O_3/CaO as the oxygen carrier for hydrogen-enriched syngas production, Chem. Eng. J. 379 (2020) 122346.
[27] L. Xu, J. Wang, Z. Li, N. Cai, Experimental study of cement-supported CuO oxygen carriers in chemical looping with oxygen uncoupling (CLOU), Energy Fuel. 27 (2013) 1522–1530.
[28] Z. Hu, M. Wang, E. Jiang, A novel continuous reactor with shaftless spiral for chemical looping gasification and the control of operating parameters, J. Energy Inst. 93 (2020) 2084–2095.
[29] Z. Hu, X. Ma, E. Jiang, The effect of microwave pretreatment on chemical looping gasification of microalgae for syngas production, Energy Convers. Manag. 143 (2017) 513–521.
[30] S. Maiti, J. Llorca, M. Dominguez, S. Colussi, A. Trovarelli, K.R. Priolkar, et al., Combustion synthesized copper-ion substituted $FeAl_2O_4$ ($Cu_{0.1}Fe_{0.9}Al_2O_4$): a

superior catalyst for methanol steam reforming compared to its impregnated analogue, J. Power Sources 304 (2016) 319–331.
[31] J.L. Chen, Y.H. Qiao, Y.D. Li, Promoting effects of doping ZnO into coprecipitated Ni-Al_2O_3 catalyst on methane decomposition to hydrogen and carbon nanofibers, Appl Catal a-Gen. 337 (2008) 148–154.
[32] M. Daofeng, Z. Haibo, M. Zhaojun, Z. Chuguang, Preparation method study on Fe_2O_3/Al_2O_3 oxygen carrier, J. Fuel Chem. Technol. 40 (2012) 795–802.
[33] S. Ma, S. Chen, M. Zhu, Z. Zhao, J. Hu, M. Wu, et al., Enhanced sintering resistance of Fe_2O_3/CeO_2 oxygen carrier for chemical looping hydrogen generation using core-shell structure, Int. J. Hydrogen Energy 44 (2019) 6491–6504.
[34] H. Zhen, H. Fang, L. Xinai, Z. Kun, L. Haibin, Thermodynamic analysis and experimental investigation of chemical-looping gasification of biomass with Fe-based oxygen carrier, Acta Energiae Solaris Sin. 34 (2013) 1943–1949.
[35] J. Yan, X. Chu, H. Jiao, S. Kang, Z. Lei, Z. Li, et al., Preparation and performance of Cu-based bimetallic oxygen carriers in chemical looping combustion with gaseous and solid fuels, Fuel Process. Technol. 205 (2020) 106463.
[36] Q. Guo, X. Hu, Y. Liu, W. Jia, M. Yang, M. Wu, et al., Coal chemical-looping gasification of Ca-based oxygen carriers decorated by CaO, Powder Technol. 275 (2015) 60–68.
[37] G. Liu, Y. Liao, Y. Wu, X. Ma, Synthesis gas production from microalgae gasification in the presence of Fe_2O_3 oxygen carrier and CaO additive, Appl. Energy 212 (2018) 955–965.
[38] G.-q. Wei, J. Feng, Y.-L. Hou, F.-Z. Li, W.-Y. Li, Z. Huang, et al., Ca-enhanced hematite oxygen carriers for chemical looping reforming of biomass pyrolyzed gas coupled with CO_2 splitting, Fuel 285 (2021) 119125.
[39] X. Zheng, Q. Su, W. Mi, P. Zhang, Effect of steam reforming on methane-fueled chemical looping combustion with Cu-based oxygen carrier, Int. J. Hydrogen Energy 39 (2014) 9158–9168.
[40] C.R. Forero, P. Gayán, L.F. de Diego, A. Abad, F. García-Labiano, J. Adánez, Syngas combustion in a 500 Wth Chemical-Looping Combustion system using an impregnated Cu-based oxygen carrier, Fuel Process. Technol. 90 (2009) 1471–1479.
[41] M.M. Yung, W.S. Jablonski, K.A. Magrini-Bair, Review of catalytic conditioning of biomass-derived syngas, Energy Fuel. 23 (2009) 1874–1887.
[42] F. He, Z. Huang, G. Wei, K. Zhao, G. Wang, X. Kong, et al., Biomass chemical-looping gasification coupled with water/CO_2-splitting using $NiFe_2O_4$ as an oxygen carrier, Energy Convers. Manag. 201 (2019) 112157.